JARO
Journal of the Association for Research in Otolaryngology

Research Article

Tumor Necrosis Factor-alpha-mutant Mice Exhibit High Frequency Hearing Loss

Naoki Oishi,[2] Jun Chen,[1] Hong-Wei Zheng,[1] Kayla Hill,[1] Jochen Schacht,[2] and Su-Hua Sha[1]

[1]*Department of Pathology and Laboratory Medicine, Medical University of South Carolina, Walton Research Building, Room 403-E, 39 Sabin Street Charleston, SC 29425, USA*
[2]*Kresge Hearing Research Institute, Department of Otolaryngology, University of Michigan, Ann Arbor, MI 48109-5616, USA*

ABSTRACT

Exogenous tumor necrosis factor-alpha (TNF-α) plays a role in auditory hair cell death by altering the expression of apoptosis-related genes in response to noxious stimuli. Little is known, however, about the function of TNF-α in normal hair cell physiology. We, therefore, investigated the cochlear morphology and auditory function of TNF-α-deficient mice. Auditory evoked brainstem response showed significantly higher thresholds, especially at higher frequencies, in 1-month-old TNF-$\alpha^{-/-}$ mice as compared to TNF-$\alpha^{+/-}$ and wild type (WT); hearing loss did not progress further from 1 to 4 months of age. There was no difference in the gross morphology of the organ of Corti, lateral wall, and spiral ganglion cells in TNF-$\alpha^{-/-}$ mice compared to WT mice at 4 months of age, nor were there differences in the anatomy of the auditory ossicles. Outer hair cells were completely intact in surface preparations of the organ of Corti of TNF-$\alpha^{-/-}$ mice, and synaptic ribbon counts of TNF-$\alpha^{-/-}$ and WT mice at 4 months of age were similar. Reduced amplitudes of distortion product otoacoustic emissions, however, indicated dysfunction of outer hair cells in TNF-$\alpha^{-/-}$ mice. Scanning electron microscopy revealed that stereocilia were sporadically absent in the basal turn and distorted in the middle turn. In summary, our results demonstrate that TNF-α-mutant mice exhibit early hearing loss, especially at higher frequencies, and that loss or malformation of the stereocilia of outer hair cells appears to be a contributing factor.

Keywords: TNF-alpha-deficient mice, higher frequency hearing loss, malformation of the stereocilia of outer hair cells

INTRODUCTION

Tumor necrosis factor-alpha (TNF-α) is a potent cytokine mediating a plethora of cellular functions including normal regulatory processes, immune and inflammatory responses, and cell death (Perry et al. 2002, Vlantis and Pasparakis 2010). Constitutive TNF-α mRNA, protein, and receptor expression has been observed in the murine brain and in immature neuronal cells during development, and in the mature central nervous system. TNF-α may affect a variety of neuronal functions, including membrane potential and second-messenger signaling pathways (Pan et al. 1997, Munoz-Fernandez and Fresno 1998). Furthermore, TNF-α has been implicated in the regulation of feeding, sleeping, and other autonomic, neuroendocrine-related functions (Plata-Salaman et al. 1988, Pan et al. 1997, Krueger et al. 1998). Increased levels of TNF-α, as well as of other cytokines, have been well documented in the pathophysiology of disease. For example, under ischemic and hemorrhagic conditions, TNF-α levels correlate with the extent of neuronal damage (Mayne et al. 2001). In Alzheimer's disease, amyloid plaques stimulate a toxic level of TNF-α production from microglial cells, while increased TNF-α expression in multiple sclerosis leads to the destruction of oligodendrocytes (Munoz-Fernandez and Fresno 1998). Attesting to its multifaceted functions, TNF-α has

Naoki Oishi and Jun Chen contributed equally to this work.

Correspondence to: Su-Hua Sha • Department of Pathology and Laboratory Medicine • Medical University of South Carolina • Walton Research Building, Room 403-E, 39 Sabin Street Charleston, SC 29425, USA. Telephone: +1-843-7928324; fax: +1-843-7920368; email: shasu@musc.edu

also been suggested to play a protective role in neurodegenerative diseases. TNF receptor (TNFR) knockout mice sustain increased cerebral damage compared to their wild type (WT) counterparts in models of ischemia and multiple sclerosis (Bruce et al. 1996, Kassiotis and Kollias 2001).

In the inner ear, the release of pro-inflammatory cytokines is triggered by noxious insults such as acoustic trauma or ototoxic drugs. Specifically, TNF-α is produced by spiral ligament fibrocytes, outer hair cells, and supporting cells within the organ of Corti following noise exposure, excessive vibration, or treatment with cisplatin (Zou et al. 2005, Fujioka et al. 2006, Moon et al. 2006, So et al. 2007, Park et al. 2009). Further supporting a pro-inflammatory role for TNF-α in cochlear injury and repair is the fact that the infusion of TNF-α into the guinea pig cochlea leads to the infiltration of inflammatory cells, such as leukocytes, and that the number of cochlear macrophages increases following acoustic trauma (Hirose et al. 2005, Keithley et al. 2008).

The induction of cell death pathways in the inner ear may also be accompanied by TNF-α release, in agreement with its potential role in the regulation of cell death via downstream targets such as nuclear factor-kappaB (NF-κB), and mitogen-activated protein kinase (MAPK), (Yang et al. 2002). Exogenous TNF-α treatment up-regulates pro-apoptotic Bax, down-regulates anti-apoptotic Bcl-2 and Bcl-X_L, and induces hair cell death in organ of Corti explants (Dinh et al. 2008). Likewise, rat organ of Corti explants challenged with TNF-α demonstrated ototoxicity accompanied by high levels of phosphorylated c-Jun N-terminal kinase, cleaved caspase-3, apoptosis-inducing factor cluster formation, and translocation of the apoptotic marker endonuclease G to the nuclei of hair cells (Bas Infante et al. 2012). The activation of caspase-3 was also seen in the UB-OC1 auditory cell line undergoing apoptosis following treatment with TNF-α (Park et al. 2012). Conversely, co-treatment with dexamethasone rescued TNF-α-induced apoptosis by down-regulating pro-apoptotic genes such as TNF receptor 1 (Van De Water et al. 2010). TNF-α has also been suggested to play a role in ischemic hearing loss, as TNF-α treatment reduced both cochlear blood flow and capillary diameter in spiral ligament capillaries and spiral modiolar arteries of guinea pigs (Scherer et al. 2010). Finally, TNF-α has also been implicated to play a role in age-related hearing loss, linking increased TNF-α to several types of cochlear pathologies (Tadros et al. 2008).

In contrast to the established involvement of TNF-α in cochlear pathology, little is known about its role in normal hair cell function. In order to gain more insight into a physiological role of TNF-α, we investigated the cochlear morphology and auditory function of commercially available TNF-α-deficient mice.

MATERIALS AND METHODS

Animals

B6.129S6-Tnf^{tm1Gkl}/J TNF-α-deficient mice (TNF-α$^{-/-}$) were purchased from The Jackson Laboratory (#005540). TNF-α-deficient mice survive gestation and homozygous mutants carry no apparent phenotypic abnormalities (Pasparakis et al. 1996).

TNF-α$^{-/-}$ mice were bred with WT mice to yield TNF-α-heterozygous (TNF-α$^{+/-}$) offspring. All mice had free access to water and a regular mouse diet (Purina 5025, St. Louis, MO), and were kept at 22 ± 1 °C under a 12:12 h light–dark cycle for acclimation for 1 week prior to the experiments. All research protocols were approved by the Institutional Animal Care and Use Committee at the Medical University of South Carolina (MUSC). Animal care was under the supervision of the Division of Laboratory Animal Resources at MUSC.

Auditory brainstem responses

Mice were anesthetized with an intra-peritoneal injection of xylazine (10 mg/kg) and ketamine (100 mg/kg), and then placed in a sound-isolated and electrically shielded booth (Acoustic Systems, Austin, TX). Body temperature was monitored and maintained near 37 °C with a heating pad. Acoustic stimuli were delivered monaurally to a Beyer earphone attached to a customized plastic speculum inserted into the ear canal. Subdermal electrodes were inserted at the vertex of the skull, under the left ear, and under the right ear (ground). Auditory brainstem responses (ABRs) were measured either at 6, 12, and 24 kHz or at 8, 16, and 32 kHz. Tucker-Davis Technologies (TDT, Alachua, FL) System III hardware and SigGen/Biosig software were used to present the stimuli (15 ms duration tone bursts with 1 ms rise–fall time) and record the response. Up to 1,024 responses were averaged for each stimulus level. The starting (and highest) intensity for ABR recordings was 100 dB sound pressure level (SPL). Thresholds were determined for each frequency by reducing the intensity in 10 dB increments and then in 5 dB steps near threshold until no organized responses were detected. Thresholds were estimated between the lowest stimulus level where a response was observed and the highest level is without response. All ABR measurements were conducted by the same experimenter who was blinded to the treatment conditions.

Distortion product otoacoustic emissions

Animals were anesthetized with ketamine (65 mg/kg), xylazine (3.5 mg/kg), and acepromazine (2 mg/kg). Body temperature was maintained through the use of water-circulating heating pads and heat lamps. Additional anesthetic (ketamine and xylazine) was administered if

needed to maintain anesthesia depth sufficient to insure immobilization and relaxation. The primary tones, F1 and F2, were set at a F2/F1 ratio of 1.2. The intensity of F1 (L1) was varied in 5 or 10 dB steps (with the intensity of F1 ranging from 10–80 dB SPL), and the intensity of F2 (L2) was maintained 10 dB lower than L1. The distortion product otoacoustic emission (DPOAE) was measured at 2F1–F2. Tones were presented via two EC1 drivers (TDT, with an aluminum-shielded enclosure made in-house) connected through separate tubes to the ear along with an electret condenser microphone (Knowles Acoustics, Itasca, IL, type FG-23329-P07, in a custom-fabricated coupler with custom-fabricated amplifier). TDT System III hardware and SigGen/BioSig software were used to present the stimuli and record responses. Continuous stimulus tones were calibrated with an 8-in. condenser microphone (Bruel and Kjaer type 4138) coupled to a volume approximating the mouse ear canal. The response curve for the electret microphone was generated in the same volume to generate conversion constants relative to the 8-in. microphone.

Histologic preparation and spiral ganglion cell counts

Mice were decapitated and their bullae rapidly removed. The cochleae were fixed with 4 % paraformaldehyde in phosphate buffer (pH 7.4) for 24 h followed by rinse in phosphate buffered saline (PBS). Cochleae were then decalcified in 5 % EDTA in PBS at room temperature for 24 h, dehydrated through a graded series of alcohols, and then processed for embedding into JB-4 Plus, a glycol methacrylate plastic. Five-micron plastic sections were cut in a paramodiolar plane and the mid-modiolar sections were identified and placed on a slide. Sections were rehydrated, and the slides dipped in Paragon for 1 min, dehydrated in graded strengths of ethanol, dipped in Xylene and coverslipped with Permount mounting medium.

Twelve mid-modiolar sections were selected and every other section was quantitatively assessed. Each selected slide was placed under the microscope and digital images acquired into a MetaMorph Image Analysis workstation under bright field optics. The most basal profile of the Rosenthal's canal was acquired at a low (×2.5–10) magnification and its outline was circled to determine the total area using the MetaMorph image analysis software. Magnification was then increased (×16–25) for counting of spiral ganglion cells (SGCs). The remaining two more apical profiles were assessed separately. For inclusion into the count, a spiral ganglion neuron had to meet the criteria of having a diameter of 12 to 15 μm with a nucleus between 5 and 9 μm in diameter. Neuronal density was then calculated by dividing the number of spiral ganglion cells by the area measured. A total of six sections were evaluated for each animal.

Morphometry of stria and spiral ligament

Plastic sections were prepared as described above and images at ×25 magnification were taken from the apex, middle, and base of the cochlea. At least four sections from each cochlea were analyzed by an observer blinded to the groups. The areas of the stria vascularis and spiral ligament were measured using the MetaMorph imaging system.

Surface preparation and diaminobenzidine staining of hair cells

The temporal bones were removed immediately following euthanasia and fixed with 4 % paraformaldehyde in PBS, pH 7.4, and kept in this fixative overnight at 4 °C. The cochleae were then rinsed in PBS. Before decalcification in a 4 % solution of sodium EDTA (adjusted with HCl to pH 7.4) at 4 °C, the apical otic capsule was removed. The EDTA solution was changed daily for 3 days. Following decalcification, the cochleae were placed into 3 % hydrogen peroxide for 2.5 h to quench endogenous peroxidases. After incubation in a solution for blocking nonspecific antibody binding overnight at 4 °C, the tissues were incubated with a primary antibody rabbit polyclonal anti-myosin VII at a 1:100 dilution; (Proteus, #PTS-25-6790) for 4 days at 4 °C on a Nutator mixer, washed in PBS, and then incubated overnight at 4 °C with biotinylated goat anti-rabbit antibody at a 1:100 dilution (Vector Laboratories). Specimens were rinsed again and then incubated overnight in ABC solution (PK-4001; Vector Laboratories, Burlingame, CA). Following another wash, the cochleae were incubated in diaminobenzidine (DAB) for 3 h, as necessary, for sufficient staining intensity, followed by washing to stop the reaction. Finally, the cochleae were microdissected into the apical, middle, and basal segments and mounted on slides with Fluoromount-G mounting medium (Southern Biotech, Birmingham, AL). Images were taken with a Zeiss microscope and AxioCam MRc5 camera with Axioplan 2 imaging software. A sample size of five mice was used for each experimental group.

Scanning electron microscopy

For scanning electron microscopy (SEM) analysis, mice were anesthetized and perfusion-fixed with 2 % glutaraldehyde in 0.15-M cacodylate buffer (pH 7.4). Temporal bones were removed, cochleae exposed, and samples fixed in a solution of 3 % glutaraldehyde, 2 % paraformaldehyde, and 1 % acrolein in 0.1-M cacodylate buffer (pH 7.4). Tissues were processed using the osmium-thiocarbohydrazide method then dehydrated in increasing concentrations of ethanol and critical-point dried with CO_2 in a SamDri 790 dryer (Tousimis, Rockville, MD) before being examined
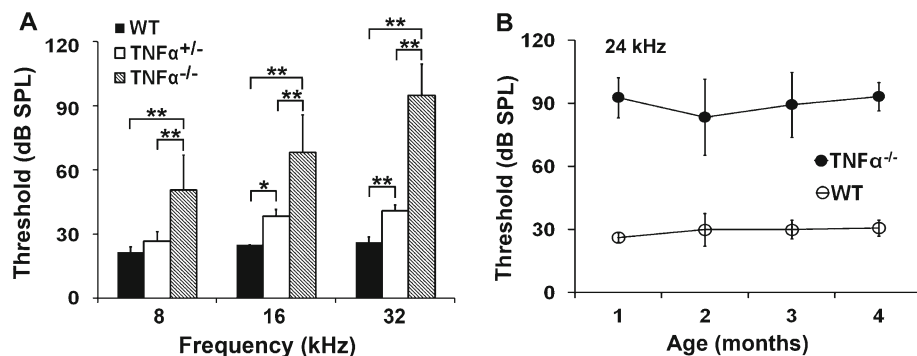
FIG. 1. TNF-α mutant mice exhibited elevated thresholds. **A** ABR thresholds of TNF-α-heterozygous (TNF-α$^{+/-}$, $n=12$), and TNF-α-deficient (TNF-α$^{-/-}$, $n=14$) mice at 1 month of age were significantly elevated at all frequencies in comparison to wild-type mice (WT, $n=8$). Data are presented as means + SD; *$P<0.045$. **$P<0.001$. **B** Auditory thresholds remained stable in both TNF-α$^{-/-}$ ($n=6$) and WT mice ($n=6$) from 1 to 4 months of age. Data are presented as means ± SD.

on an Amray 1910 Field Emission Scanning Electron Microscope and photographed digitally using XStream software.

Histologic preparation, confocal imaging, and synaptic count

For immunolabeling and quantification of synaptic ribbons, cochleae were perfused with 4 % paraformaldehyde and 0.25 % glutaraldehyde, fixed for 1 h, decalcified in EDTA, microdissected into six pieces, and immunolabeled with antibodies to C-terminal binding protein 2 (mouse anti-CtBP2 used at 1:200; BD Biosciences, San Jose, CA) and a secondary antibody coupled to Alexa Fluor 488 (Invitrogen Life Technologies, Grand Island, NY). Rhodamine phalloidin was used to image stereocilia. Confocal z-stacks were obtained using a high-resolution [1.4 numerical aperture] oil-immersion objective and ×2 digital zoom on a Leica TCS SP2. Care was taken to span the entire synaptic pole of the hair cells in the z-

dimension, with a z-step-size of 0.25 mm from the subjacent inner spiral bundle to the apical-most ribbon or nerve terminal in the supranuclear region. Image stacks were imported to image-processing software (Amira: Visage Imaging), where synaptic ribbons were counted and divided by the total number of inner hair cell nuclei in the microscopic field (including fractional estimates, when necessary, at the apical and basal ends of the image stack). To avoid underestimating ribbon counts due to superposition in the image stacks, three-dimensional renderings were produced, using the "isosurface" feature in Amira, and rotated to disambiguate the xy projection images.

Morphological analyses of auditory ossicles

Mouse skulls were fixed in 4 % paraformaldehyde. For macroscopic analysis, auditory ossicles were isolated after removing the temporal bone, and observed using a Zeiss Stemi 2000-C zoom microscope configured with the Zeiss AxioCam MRM digital camera system.
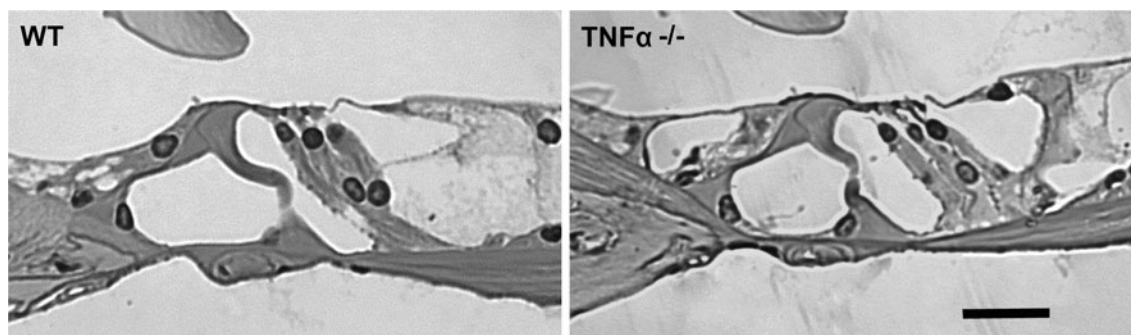
FIG. 2. Cochlear morphology of the organ of Corti in both TNF-α$^{-/-}$ and WT mice at 4 months of age. There was no significant variation in the morphology of the organ of Corti visualized in plastic sections between TNF-α$^{-/-}$ and WT mice. These images are representative of three ears analyzed for each condition. *SCALE BAR*=30 μm.

Statistical analysis

Data were statistically evaluated by one way ANOVA or repeated measures ANOVA with Tukey's multiple comparisons or two-tailed unpaired t test using IBM SPSS Statistics. A P value of <0.05 was considered statistically significant.

RESULTS

TNF-α-mutant mice exhibit stable hearing loss

TNF-α-mutant mice exhibited hearing loss at 1 month of age. The ABR thresholds of both TNF-$\alpha^{-/-}$ and TNF-$\alpha^{+/-}$ mice were significantly elevated compared to WT mice (Fig. 1A. $F_{2,31}$=79.952, P<0.001). The threshold of TNF-$\alpha^{-/-}$ was greater than WT (P<0.001) and TNF-$\alpha^{+/-}$ (P<0.001). The threshold of TNF-$\alpha^{+/-}$ was higher than WT (P=0.039). Tukey's multiple comparisons test showed a significant difference at 16 kHz between TNF-$\alpha^{-/-}$ and WT (P<0.001), TNF-$\alpha^{+/-}$ and WT (P=0.045), TNF-$\alpha^{+/-}$ and TNF-$\alpha^{-/-}$ (P<0.001), as well as 32 kHz between TNF-$\alpha^{-/-}$ and WT (P<0.001), TNF-$\alpha^{+/-}$ and WT (P=0.006), TNF-$\alpha^{+/-}$ and TNF-$\alpha^{-/-}$ (P<0.001). At 8 kHz, only the hearing thresholds of knockout mice were significantly different from wild type and heterozygous mice (TNF-$\alpha^{-/-}$ vs WT= P<0.001, TNF-$\alpha^{-/-}$ vs TNF$\alpha^{+/-}$=P<0.001). Meanwhile, thresholds of TNF-$\alpha^{-/-}$ mice at 32 kHz were significantly higher than at 8 kHz (P<0.001) and 16 kHz (P<0.001) indicating a high to low frequency gradient hearing loss.

ABR thresholds of WT mice as well as the elevated thresholds of TNF-$\alpha^{-/-}$ mice remained stable from 1 to 4 months of age ($F_{3,8}$=3.628, P=0.064). There was no significant group or age interaction ($F_{3,8}$=1.321, P=0.334). The thresholds were followed only at 24 kHz (Fig. 1B) because of the already extremely elevated thresholds of TNF-$\alpha^{-/-}$ mice at 32 kHz.

TNF-$\alpha^{-/-}$ and WT mice have similar cochlear morphology

We began delineating possible causes of the elevated ABR thresholds by examining the morphology of cochlear structures. Light microscopic evaluation of plastic sections of both TNF-$\alpha^{-/-}$ and WT mice revealed no difference in the cochlear morphology at 4 months of age, including no apparent changes in the organ of Corti (Fig. 2), spiral ganglion cells (Fig. 3), and lateral wall structures (Fig. 4). Quantification of SGC density confirmed a lack of difference between WT and TNF-α knockout mice in the basal (t_4=−0.889, P=0.424), middle (t_4=−0.997, P=0.375), and apical regions (t_4=−0.649, P=0.552). Measurement of the area of the stria (base: t_4=−0.209, P=0.845, middle t_4=−0.949, P=0.396, apex: t_4=−1.309, P=0.261) and spiral ligament (base: t_4=−0.302, P=0.778, middle: t_4=1.999, P=0.116,

apex: t_4=1.501, P=0.208) failed to show a difference between groups.
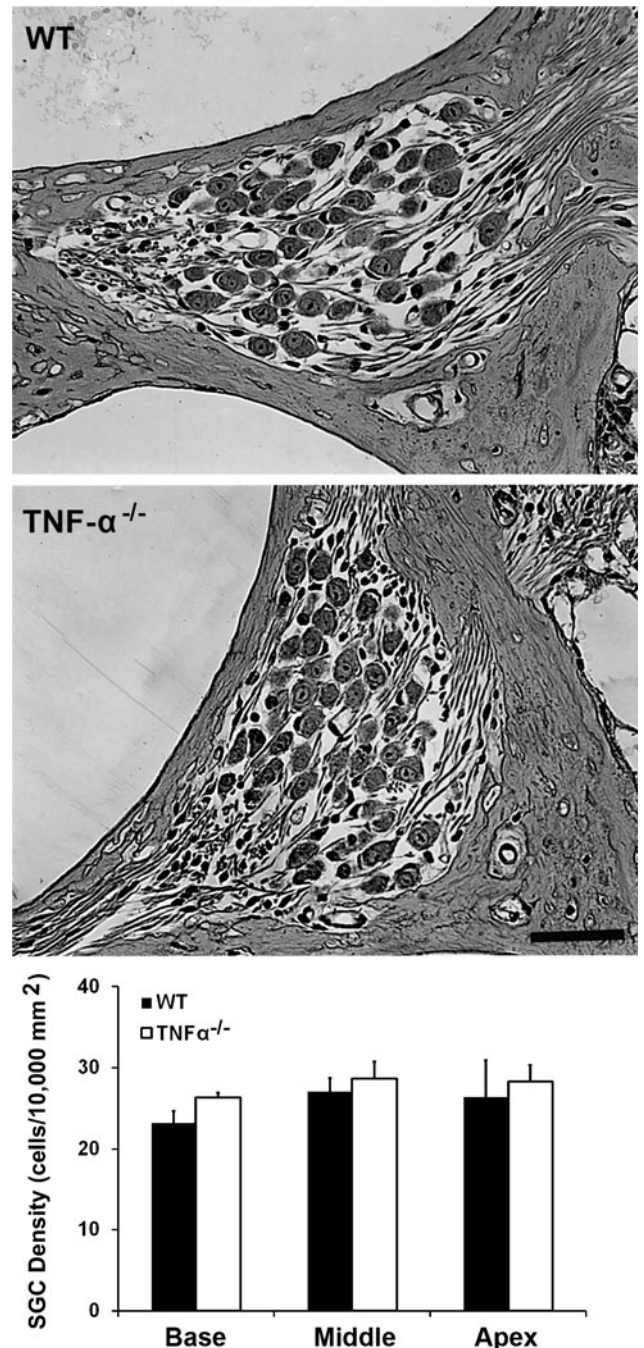
FIG. 3. Cochlear morphology of spiral ganglion cells of TNF-$\alpha^{-/-}$ and WT mice at 4 months of age. No differences were observed in the number of SGCs between TNF-$\alpha^{-/-}$ and WT mice. These images are representative of three ears analyzed for each condition. *SCALE BAR*=30 μm. Quantification of the density of spiral ganglion cells confirmed a lack of difference between the knockout and WT mice. Data are presented as means + SD, n=3 in each group.

TNF-α$^{-/-}$ and WT mice have similar auditory ossicle morphology

In the absence of gross cochlear morphological abnormalities, we examined possible defects in the ossicular chain, since TNF-α has been implicated in regulating bone turnover (Robinson et al. 2007; Schett 2011). The malleus, incus, and stapes were isolated from the middle-ear cavities of TNF-α$^{-/-}$ and WT mice at 2 months of age. There were no differences in the morphology of the auditory ossicles between TNF-α$^{-/-}$ and WT mice (Fig. 5).

TNF-α$^{-/-}$ mice display no loss of hair cells or synaptic ribbons

For a more detailed investigation into the presence or absence of hair cells, surface preparations of the cochlear epithelium from TNF-α$^{-/-}$ mice at 2 months of age were labeled with myosin VII and stained with DAB to outline outer hair cells. No outer or inner hair cell loss was observed along the entire cochlear epithelium in TNF-α$^{-/-}$ mice (Fig. 6A and 6B). In addition, the synaptic ribbons at the inner hair cell synapse were immunolabeled with anti-CtBP2 (Fig. 6C) at 4 months of age. There was no significant difference in the number of ribbons between TNF-α$^{-/-}$ and WT mice in the apex, middle, and basal regions of the cochlea. The average number of ribbons in the basal region was approximately 15 in both TNF-α$^{-/-}$ and WT mice.

TNF-α-mutant mice show aberrant DPOAE

For further analysis of auditory performance, we conducted DPOAE measurements in the animals used for ABR testing (Fig. 1B) at 4 months of age, the termination of the ABR study. DPOAE 2F1–F2 emission amplitude thresholds were significantly elevated in TNF-α$^{-/-}$ mice compared to WT mice at 12 kHz ($F_{1,10}=12.36$, $P=0.006$) and 24 kHz ($F_{1,10}=59.766$, $P<0.001$), but not at 6 kHz ($F_{1,10}=4.432$, $P=0.062$) (Fig. 7).

TNF-α$^{-/-}$ mice display stereocilia defects

Following on the observation of functionally defective outer hair cells, we performed scanning electron microscopy of the cochleae of TNF-α$^{-/-}$ and WT mice of 2 months of age for detailed visualization of inner and outer hair cell stereocilia. Stereocilia on outer hair cells in the basal turn of the organ of Corti of TNF-α$^{-/-}$ mice were missing sporadically, and collapsed stereocilia were observed in the middle turn (Fig. 8). Stereocilia on inner hair cells appeared normal.
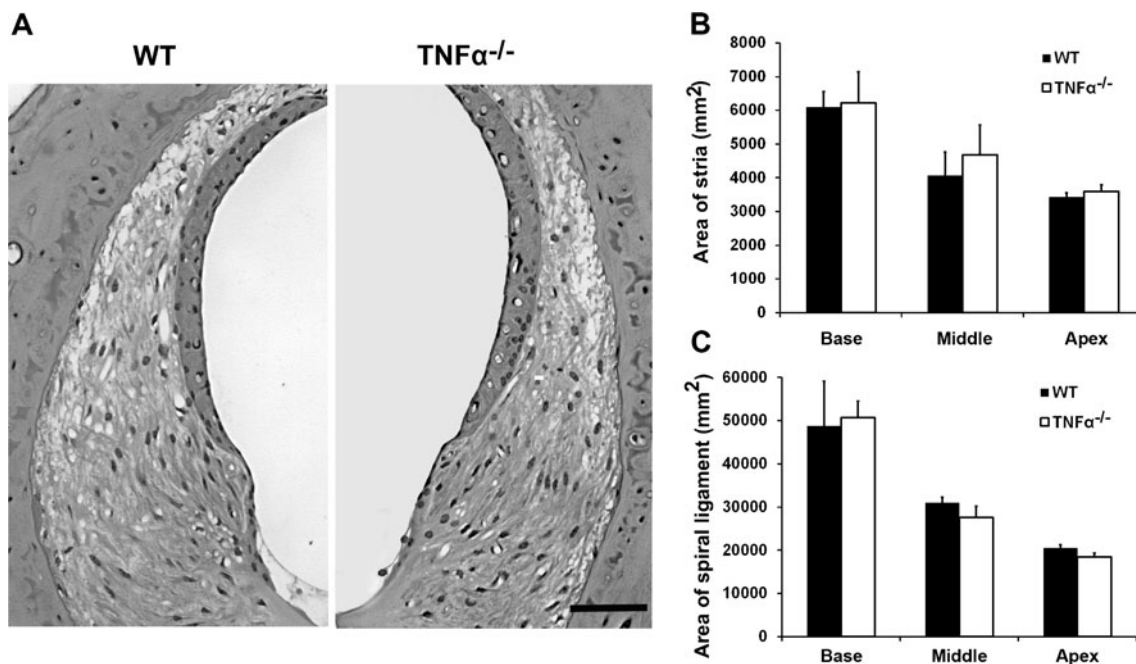

FIG. 4. Cochlear morphology of the lateral wall structures of TNF-α$^{-/-}$ and WT mice at 4 months of age. The lateral wall structures of TNF-α$^{-/-}$ and WT mice appear similar. The images are representative of three ears analyzed for each condition. *SCALE* *BAR*=30 μm. Quantification of the areas of the stria and spiral ligament showed no significant difference between knockout and WT mice. Data are presented as means + SD, *n*=3 in each group.
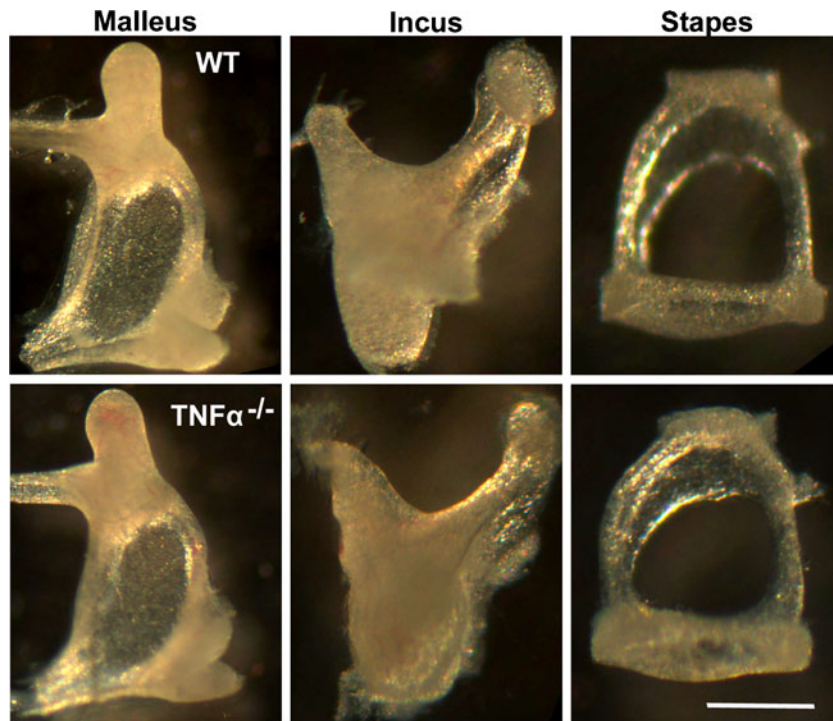
FIG. 5. Ossicular morphology of TNF-α$^{-/-}$ mice compared to WT mice. Analysis of the morphology of the malleus, incus, and stapes revealed no differences between TNF-α$^{-/-}$ and WT mice at 2 months of age. The images are representative of three ears for each condition. *SCALE BAR*=500 μm.
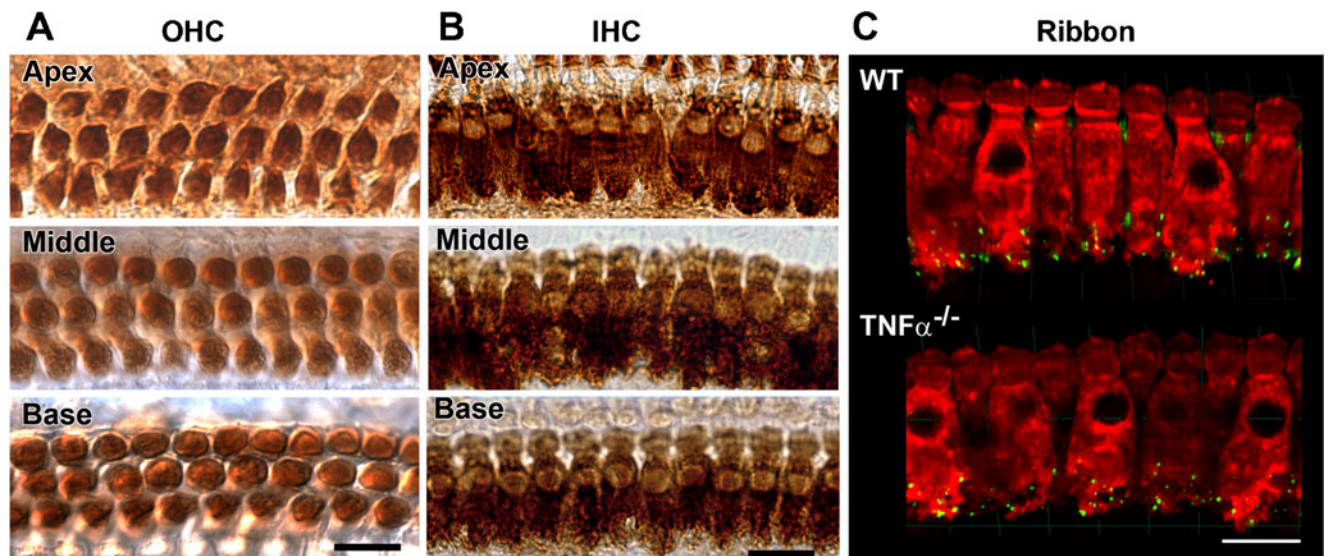
FIG. 6. Morphological features of sensory hair cells and *IHC* synaptic ribbons in TNF-α$^{-/-}$ mice. Representative images from DAB-stained cochlear sensory epithelia of TNF-α$^{-/-}$ mice at 2 months of age showed no outer hair cell (*OHC*) (**A**) or inner hair cell (*IHC*) (**B**) loss in the apical, middle, and basal regions. These images are representative of three ears under each condition. *SCALE BAR*= 10 μm. **C** *IHC* synaptic ribbons. Synaptic ribbons were immunolabeled with CtBP2 antibody (*GREEN*). Quantification of synaptic ribbons in the basal region revealed no significant difference between TNF-α$^{-/-}$ and WT mice at 4 months of age. Rhodamine phalloidin (*RED*) was used to label F-actin of sensory cells. These images are representative of four cochleae analyzed for each condition. *SCALE BAR*=20 μm.
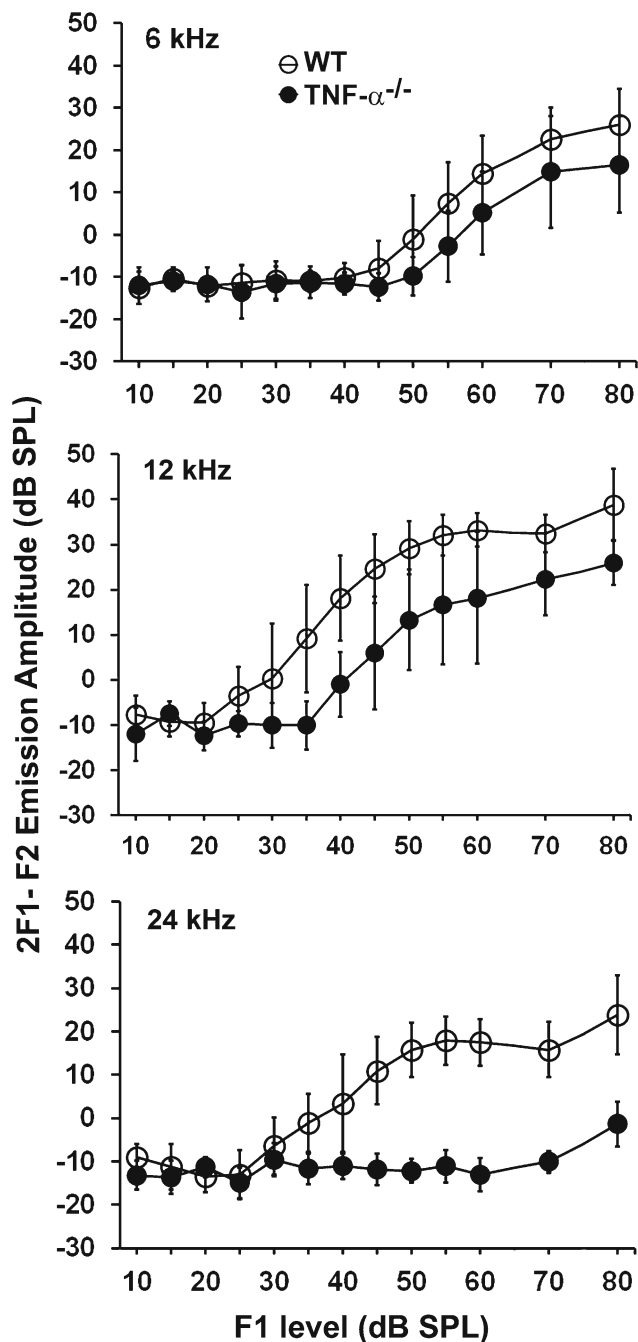
FIG. 7. DPOAE amplitudes were significantly decreased in TNF-$\alpha^{-/-}$ mice at 12 and 24 kHz, but not at 6 kHz. The DPOAE measurements were taken at 4 months of age from the animals used for the longitudinal ABR study (Fig. 1B). Data are presented as means ± SD, $n=6$.

DISCUSSION

Our results provide evidence that TNF-α is required for normal development and function of the cochlea. Congenital deficit of TNF-α causes malformation of outer hair cell stereocilia primarily in the lower turns of

the cochlea, resulting in hearing loss at high frequencies that is more severe in TNF-$\alpha^{-/-}$ than in TNF-$\alpha^{+/-}$ mice.

Hearing loss as a result of TNF-α deficiency seems counterintuitive. Generally, it is an increase in TNF-α signaling, either secondary to disease or via pharmacological manipulation, that will cause loss of hair cells or auditory function, while blocking TNF-α affords protection in both human and animal models. Patients with idiopathic sensorineural hearing loss who did not respond to drug treatment maintained higher blood levels of TNF-α than positive responders (Demirhan et al. 2013). Autoimmune sensorineural hearing loss was also attenuated by TNF-α blockers in a prospective pilot study (van Wijk et al. 2006). In animal models, noise-overstimulation elevated TNF-α and other pro-inflammatory cytokines in the rat cochlea (Fujioka et al. 2006), while drugs preventing TNF-α expression prevented loss of outer hair cells following intense noise treatment (Bas et al. 2009 In cochlear explants, TNF-α was upregulated by hypoxia, a condition that can lead to hearing loss (Khan et al. 2010). Likewise, direct application of TNF-α to cultures of the organ of Corti confirms its toxic effects on hair cells (Haake et al. 2009).

Despite the manifold potential actions of TNF-α, the auditory consequences of its deficiency seem highly specific to the cochlea. The absence of gross morphological changes is well in line with the fact that TNF-α-deficient mice show no apparent phenotype (Pasparakis et al. 1996). Prompted by our initial observation of apparently intact hair cells, and given the broad range of TNF-α functions, we deemed it necessary to explore potential sites of damage from the middle ear to the cochlea and the cochlear nerve in order to search for the most likely sites of action.

TNF-α and other TNF family members can regulate osteoclast formation and bone turnover via several TNF-receptors that are also expressed by osteoblasts and osteoblast precursors (Robinson et al. 2007). TNF-α is a major trigger for bone loss (Schett 2011) and therefore might affect bone homeostasis in TNF-α-deficient mice, influencing middle-ear conduction. This possibility is underscored by the observation that osteoclastic resorption of middle ear bones is increased in mice lacking osteoprotegerin (Kanzaki et al. 2006). Normally, osteoprotegerin would inactivate signaling via receptor activator of NF-κB, a member of the tumor necrosis factor family, by acting as a decoy ligand for receptor activator of NF-κB ligand, and thereby preventing its osteoclastic activity. However, the lack of obvious visualized ossicular morphological changes rules out an imbalance of middle ear bone homeostasis.

Enhanced activity of TNF-α has been associated with vascular dysfunction in a variety of pathologies, mostly in connection with inflammatory conditions
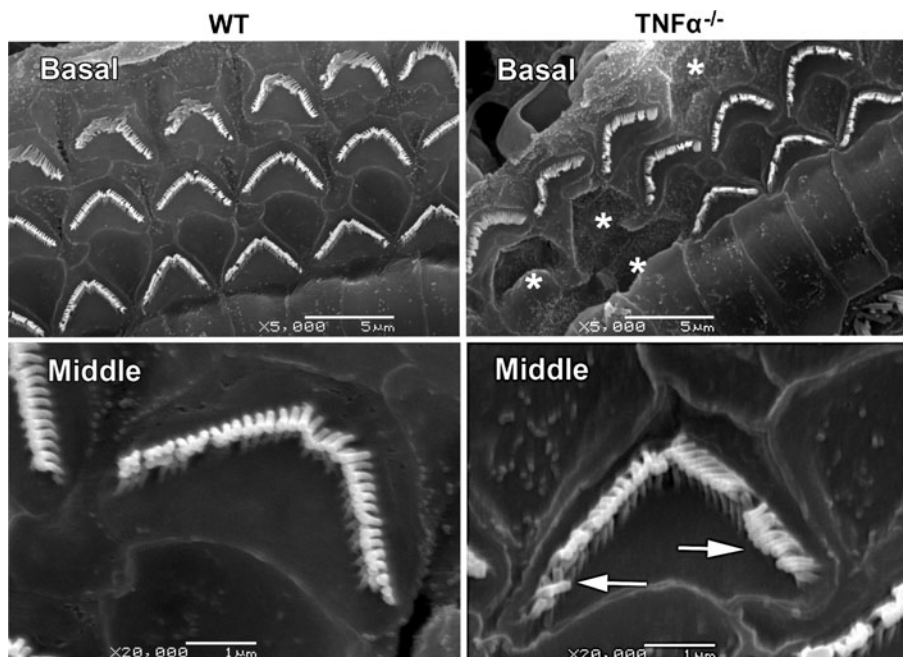
FIG. 8. Morphological features of outer hair cell stereocilia at 2 months of age. Scanning electron microscopy revealed sporadic stereocilia loss (*WHITE ASTERISKS*) in the basal turns of TNF-α^{−/−} mice. Additionally, collapsed stereocilia (*ARROWS*) were observed in the middle turns. Corresponding stereocilia of WT mice appeared normal. The images are representative of three ears under each condition. *SCALE BAR*=5 μm for the images of the base and 1 μm for those of the middle turn.

(Kleinbongard et al. 2010). In the inner ear, the lateral wall tissues (spiral ligament, spiral limbus, and fibrocytes) are among the major sites of TNF-α expression (Ichimiya et al. 2000; So et al. 2007) and the application of TNF-α can reduce capillary diameter and blood flow throughout the cochlear microvasculature (Scherer et al. 2010). The absence of TNF-α in our mouse model, in contrast, had no influence on the gross morphology of the lateral wall tissues.

TNF-α is also an important mediator of non-inflammatory diseases and participates in maintaining the balance between neuronal preservation and death in response to potentially neurotoxic insults (Cheng et al. 1994; Stoll et al. 2000) including glutamate-induced excitotoxicity (Marchetti et al. 2004), a condition that can occur at the inner hair cell synapse after ischemia or acoustic overstimulation (Pujol and Puel 1999). Its function in neuroprotection and plasticity may be mediated by tumor necrosis factor receptor-2 (TNFR2) and the activation of downstream pathways involving NF-κB (Dolga et al. 2008; Pradillo et al. 2009). TNFR2 is widely induced in structures of the mature cochlea after noxious stimuli (Zou et al. 2005) and the NF-κB pathway is protective against ototoxic insults to the cochlea (Jiang et al. 2005). In the absence of overt stress, however, the TNF-α knock-out mice in this study showed normal synapses and neurons.

Thus, despite the potential for multiple targets of injury, the cochlear defect of TNF-α-deficient mice is localized to outer hair cells. This is suggested by abnormal DPOAE, an indicator of outer hair cell function, and confirmed by the observation under electron microscopy of missing or collapsed stereocilia on these cells. How TNF-α relates to the structural integrity of cochlear stereocilia remains speculative and we are not aware of any studies that address this question. Casting a wider net, however, we might draw some conjecture from pathways regulated by TNF-α and related cytokines that are involved in ciliogenesis and ciliopathies (Sharma et al. 2008). In particular, the tumor necrosis factor-alpha receptor 3-interacting protein (Traf3ip1), which couples receptor activation to downstream pathways, is localized to cilia in several species and its deficiency causes defects in mammalian ciliogenesis (Berbari et al. 2011). Although the structure of cilia is distinctly different from that of stereocilia, it is intriguing that Traf3ip1 can also interact with actin and tubulin (Guo et al. 2010), components of stereocilia and the cuticular region of outer hair cells. Hence, Traf3ip1 and, by implication, TNF-α may play a yet to be elucidated role in the structural dynamics of stereocilia.

ACKNOWLEDGMENTS

REFERENCES

Bas Infante E, Channer GA, Telischi FF, Gupta C, Dinh JT, Vu L, Eshraghi AA, Van De Water TR (2012) Mannitol protects hair cells against tumor necrosis factor alpha-induced loss. Otol Neurotol 33:1656–1663. doi:10.1097/MAO.0b013e31826bedd9

Bas E, Martinez-Soriano F, Lainez JM, Marco J (2009) An experimental comparative study of dexamethasone, melatonin and tacrolimus in noise-induced hearing loss. Acta Otolaryngol 129:385–389

Berbari NF, Kin NW, Sharma N, Michaud EJ, Kesterson RA, Yoder BK (2011) Mutations in Traf3ip1 reveal defects in ciliogenesis, embryonic develoment, and altered cell size regulation. Dev Biol 360:66–76

Bruce AJ, Boling W, Kindy MS, Peschon J, Kraemer PJ, Carpenter MK, Holtsberg FW, Mattson MP (1996) Altered neuronal and microglial responses to excitotoxic and ischemic brain injury in mice lacking TNF receptors. Nat Med 2:788–794

Cheng B, Christakos S, Mattson MP (1994) Tumor necrosis factors protect neurons against metabolic-excitotoxic insults and promote maintenance of calcium homeostasis. Neuron 12:139–153

Demirhan E, Eskut NP, Zorlu Y, Cukurova I, Tuna G, Kirkali FG (2013) Blood levels of TNF-a, IL-10, and IL-12 in idiopathic sudden sensorineural hearing loss. Laryngoscope 123:1778–1781. doi:10.1002/lary.23907

Dinh CT, Haake S, Chen S, Hoang K, Nong E, Eshraghi AA, Balkany TJ, Van De Water TR (2008) Dexamethasone protects organ of corti explants against tumor necrosis factor-alpha-induced loss of auditory hair cells and alters the expression levels of apoptosis-related genes. Neuroscience 157:405–413

Dolga AM, Granic I, Blank T, Knaus HG, Spiess J, Luiten PG, Eisel UL, Nijholt IM (2008) TNF-alpha-mediates neuroprotection against glutamate-induced excitotoxicity via NF-kappaB-dependent up-regulation of K2.2 channels. J Neurochem 107:1158–1167

Fujioka M, Kanzaki S, Okano HJ, Masuda M, Ogawa K, Okano H (2006) Proinflammatory cytokines expression in noise-induced damaged cochlea. J Neurosci Res 83:575–583

Guo CW, Xiong S, Liu G, Wang YF, He QY, Zhang XE, Zhang ZP, Ge F, Kitazato K (2010) Proteomic analysis reveals novel binding partners of MIP-T3 in human cells. Proteomics 10:2337–2347

Haake SM, Dinh CT, Chen S, Eshraghi AA, Van De Water TR (2009) Dexamethasone protects auditory hair cells against TNFalpha-initiated apoptosis via activation of PI3K/Akt and NFkappaB signaling. Hear Res 255:22–32

Hirose K, Discolo CM, Keasler JR, Ransohoff R (2005) Mononuclear phagocytes migrate into the murine cochlea after acoustic trauma. J Comp Neurol 489:180–194

Ichimiya I, Yoshida K, Hirano T, Suzuki M, Mogi G (2000) Significance of spiral ligament fibrocytes with cochlear inflammation. Int J Pediatr Otorhinolaryngol 56:45–41

Jiang H, Sha S-H, Schacht J (2005) The NF-κB pathway protects cochlear hair cells from aminoglycoside-induced ototoxicity. J Neurosci Res 79:644–651

Kanzaki S, Ito M, Takada Y, Ogawa K, Matsuo K (2006) Resorption of auditory ossicles and hearing loss in mice lacking osteoprotegerin. Bone 39:414–419

Kassiotis G, Kollias G (2001) Uncoupling the proinflammatory from the immunosuppressive properties of tumor necrosis factor (TNF) at the p55 TNF receptor level: implications for pathogenesis and therapy of autoimmune demyelination. J Exp Med 193:427–434

Keithley EM, Wang X, Barkdull GC (2008) Tumor necrosis factor alpha can induce recruitment of inflammatory cells to the cochlea. Otol Neurotol 29:854–859

Khan M, Szczepek AJ, Haupt H, Olze H, Masurek B (2010) Expression of the proinflammatory cytokines in cochlear explant cultures: influence of normoxia and hypoxia. Neurosci Lett 479:249–452

Kleinbongard P, Heusch G, Schulz R (2010) TNFalpha in atherosclerosis, myocardial ischemia/reperfusion and heart failure. Pharmacol Ther 127:295–314

Krueger JM, Fang J, Taishi P, Chen Z, Kushikata T, Gardi J (1998) Sleep. A physiologic role for IL-1 beta and TNF-alpha. Ann N Y Acad Sci 856:148–159

Marchetti L, Klein M, Schlett KI, Pfizenmaier K, Eisel UL (2004) Tumor necrosis factor (TNF)-mediated neuroprotection against glutamate-induced excitotoxicity is enhanced by N-methyl-D-aspartate receptor activation. Essential role of a TNF receptor 2-mediated phosphatidylinositol 3-kinase-dependent NF-kappa B pathway. J Biol Chem 279:32869–32881

Mayne M, Ni W, Yan HJ, Xue M, Johnston JB, Del Bigio MR, Peeling J, Power C (2001) Antisense oligodeoxynucleotide inhibition of tumor necrosis factor-alpha expression is neuroprotective after intracerebral hemorrhage. Stroke 32:240–248

Moon SK, Park R, Lee HY, Nam GJ, Cha K, Andalibi A, Lim DJ (2006) Spiral ligament fibrocytes release chemokines in response to otitis media pathogens. Acta Otolaryngol 126:564–569

Munoz-Fernandez MA, Fresno M (1998) The role of tumour necrosis factor, interleukin 6, interferon-gamma and inducible nitric oxide synthase in the development and pathology of the nervous system. Prog Neurobiol 56:307–340

Palladino MA, Bahjat FR, Theodorakis EA, Moldawer LL (2003) Anti-TNF-alpha therapies: the next generation. Nat Rev Drug Discov 2:736–746

Pan W, Zadina JE, Harlan RE, Weber JT, Banks WA, Kastin AJ (1997) Tumor necrosis factor-alpha: a neuromodulator in the CNS. Neurosci Biobehav Rev 21:603–613

Park HJ, Kim HJ, Bae GS, Seo SW, Kim DY, Jung WS, Kim MS, Song MY, Kim EK, Kwon KB, Hwang SY, Song HJ, Park CS, Park RK, Chong MS, Park SJ (2009) Selective GSK-3beta inhibitors attenuate the cisplatin-induced cytotoxicity of auditory cells. Hear Res 257:53–62

Park HY, Lee MH, Kang SU, Hwang HS, Park K, Choung YH, Kim CH (2012) Nitric oxide mediates TNF-alpha-induced apoptosis in the auditory cell line. Laryngoscope 122:2256–2264

Pasparakis M, Alexopoulou L, Episkopou V, Kollias G (1996) Immune and inflammatory responses in TNF alpha-deficient mice: a critical requirement for TNF alpha in the formation of primary B cell follicles, follicular dendritic cell networks and germinal centers, and in the maturation of the humoral immune response. J Exp Med 184:1397–1411

Perry SW, Dewhurst S, Bellizzi MJ, Gelbard HA (2002) Tumor necrosis factor-alpha in normal and diseased brain: conflicting effects via intraneuronal receptor crosstalk? J Neurovirol 8:611–624

Plata-Salaman CR, Oomura Y, Kai Y (1988) Tumor necrosis factor and interleukin-1 beta: suppression of food intake by direct action in the central nervous system. Brain Res 448:106–114

Pradillo JM, Fernandez-Lopez D, Garcia-Yebenes I, Sobrado M, Hurtado O, Moro MA, Lizasoain I (2009) Toll-like receptor 4 is involved in neuroprotection afforded by ischemic preconditioning. J Neurochem 109:287–294

Pujol R, Puel JL (1999) Excitotoxicity, synaptic repair, and functional recovery in the mammalian cochlea: a review of recent findings. Ann N Y Acad Sci 884:249–254

Robinson LJ, Borysenko CW, Blair HC (2007) Tumor necrosis factor family receptors regulating bone turnover: new observations in osteoblastic and osteoclastic cell lines. Ann N Y Acad Sci 1116:432–443

Scherer EQ, Yang J, Canis M, Reimann K, Ivanov K, Diehl CD, Backx PH, Wier WG, Strieth S, Wangemann P, Voigtlaender-Bolz J, Lidington D, Bolz SS (2010) Tumor necrosis factor-alpha enhances microvascular tone and reduces blood flow in the cochlea via enhanced sphingosine-1-phosphate signaling. Stroke 41:2618–2624

Schett G (2011) Effects of inflammatory and anti-inflammatory cytokines on the bone. Eur J Clin Invest 41:1361–1366

Sharma N, Berbari NF, Yoder BK (2008) Ciliary dysfunction in developmental abnormalities and diseases. Curr Top Dev Biol 85:371–427

So H, Kim H, Lee JH, Park C, Kim Y, Kim E, Kim JK, Yun KJ, Lee KM, Lee HY, Moon SK, Lim DJ, Park R (2007) Cisplatin cytotoxicity of auditory cells requires secretions of proinflammatory cytokines via activation of ERK and NF-kappaB. J Assoc Res Otolaryngol 8:338–355

Stoll G, Jander S, Schroeter M (2000) Cytokines in CNS disorders: neurotoxicity versus neuroprotection. J Neural Transm Suppl 59:81–89

Tadros SF, D'Souza M, Zhu X, Frisina RD (2008) Apoptosis-related genes change their expression with age and hearing loss in the mouse cochlea. Apoptosis 13:1303–1321

Van De Water TR, Abi Hachem RN, Dinh CT, Bas E, Haake SM, Hoosien G, Vivero R, Chan S, He J, Eshraghi AA, Angeli SI, Telischi FF, Balkany TJ (2010) Conservation of hearing and protection of auditory hair cells against trauma-induced losses by local dexamethasone therapy: molecular and genetic mechanisms. Cochlear Implants Int 11(Suppl 1):42–55

Van Wijk F, Staecker H, Keithley E, Lefebvre PP (2006) Local perfusion of the tumor necrosis factor alpha blocker infliximab to the inner ear improves autoimmune neurosensory hearing loss. Audiol Neurootol 11:357–365

Vlantis K, Pasparakis M (2010) Role of TNF in pathologies induced by nuclear factor kappaB deficiency. Curr Dir Autoimmun 11:80–93

Yang L, Lindholm K, Konishi Y, Li R, Shen Y (2002) Target depletion of distinct tumor necrosis factor receptor subtypes reveals hippocampal neuron death and survival through different signal transduction pathways. J Neurosci 22:3025–3032

Zou J, Pyykko I, Sutinen P, Toppila E (2005) Vibration induced hearing loss in guinea pig cochlea: expression of TNF-alpha and VEGF. Hear Res 202:13–20